Inorganic Chemistry Research

Article

Conductor-like Polarizable Continuum Model (CPCM) Solvation Analysis in a N-heterocyclic Carbene Complex of Stannocene

Simin Samavat[a], Reza Ghiasi[b,*] and Bita Mohtat[a]

[a]*Department of Chemistry, Karaj Branch, Islamic Azad University, Karaj, Iran*
[b]*Department of Chemistry, East Tehran Branch, Islamic Azad University, Tehran, Iran*

Received: September 12, 2021; Accepted: December 16, 2021
Cite This: *Inorg. Chem. Res.* **2021**, *5*, 257-264. DOI: 10.22036/icr.2021.304488.1116

Abstract: We explored solvent effect on the structural, ^{119}Sn NMR chemical shift and electronic spectrum for a N-heterocyclic carbene complex of stannocene, Cp_2SnNHC, using MPW1PW91 method. The self-consistent reaction field theory (SCRF) based on conductor-like polarizable continuum model (PCM) was used to illustrate the solvent effects. The correlations between the computed parameters and solvent polarity functions (dielectric constant (ε) and refractive index (n_D)) were provided. Correlations of the calculated spectral parameters ($\delta(^{119}Sn)$ and λ_{max}) with the Kirkwood-Bauer-Magat equation (KBM) and improved form of this equation were provided. Fukui function and dual descriptor were used to reveal the study the favorable site of electrophilic attack.

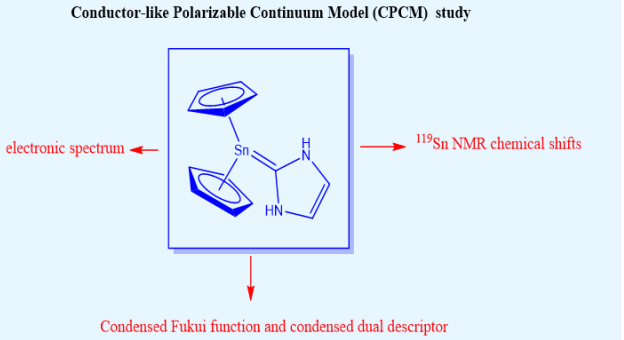

Keywords: Carbene complex, Solvent effect, ^{119}Sn NMR chemical shifts, Kirkwood-Bauer-Magat equation (KBM), Electronic spectrum

1. INTRODUCTION

Then the firstly production and separation of Wanzlick-Arduengo-type N-heterocyclic carbenes (NHCs),[1-3] they have changed into one of the most significant ligands in transition-metal chemistry.[4-6] The structure and properties of these complexes have been illustrated using computational methods. In addition, several examples of main-group metal complexes with NHCs are recognized.[7] Besides, carbenes have played a significant character in the separation of low-valent main-group compounds.[8-10] Among others, numerous germylene, stannylene, and plumbylene NHC complexes,[11-15] as well as related stannylene isonitrile complexes[16] have been reported. Yet, although NHC complexes of group 2 and 4 metallocenes are identified,[17,18] and Lewis acid-base adducts of stannocene and plumbocene with tetramethylethylenediamine and bipyridine have been described,[19,20] importance the Lewis acidic character of these metallocenes, the reactivity of group 14 metallocenes (tetrelocenes) toward NHCs is unknown. On this basis, many efforts have been done to study the reactivity of stannocenes, one of the longest recognized group 14 metallocenes, toward NHCs.

Synthesis and spectroscopic properties of the numerous stannocene carbene complexes have been reported[21] and their bonding characterization have been explored.[22]

Solvents show a noteworthy effect in chemistry and change the molecular behaviors through variations to the interactions between solvent molecules and solute.[23-25] Quantum mechanical (QM) calculations have been employed to explore the solvent effect in the electronic structure.[26,27] Numerous papers have been published about of solvent effect on the structural, electronic and spectroscopic properties of inorganic and organometallic complexes.[28-44]

As a part of our research on the solvent effect on the structure and properties of the organometallic complexes, in this paper, we studied the influence of solvent polarity on the structure, electronic, reactivity, electronic spectrum and ^{119}Sn NMR chemical shifts of Cp_2Sn=NHC complex.

2. COMPUTATIONAL METHOD

The software package of Gaussian 09 was used for conducting all calculations[45]. The standard 6-311G(d,p) basis set[46-49] was considered for C, H, N, and O, while the Sn element was described by the Def2-TZVPPD basis set.[50] Pseudo-potential effective core potential (ECP) was applied to the Def2-TZVPPD basis set[51] to exclude direct

calculation of the exchange and correlation integrals related to 28 electrons of the Sn atom.

One-parameter hybrid functional with adapted Perdew-Wang exchange and correlation (MPW1PW91) is used for optimizations of the studied molecules.[52] MPW1PW91 functional revealed better results in the transition metal complexes in compared to B3LYP.[53-56] Harmonic vibrational frequencies demonstrated that the optimized molecules have no imaginary frequency.

To determine the effects of geometric structures on electronic and optical properties, first, the Hirshfeld population analysis was performed based on optimized structures. This analysis is a very general atomic population way established on deformation density partition.[57] Hirshfeld atomic charges were calculated using the Multiwfn 3.5 package.[58]

To study the solvation impacts, we utilized a self-consistent reaction field (SCRF) method, in particular using the conductor-like polarizable continuum model (CPCM).[59, 60]

The theoretical study of the solvent-induced λ_{max} shifts is considered by Kirkwood-Bauer-Magat equation (KBM):[61]

$$\frac{(\lambda_{max,gas} - \lambda_{max,solution})}{\lambda_{max,gas}} = \frac{\Delta\lambda_{max}}{\lambda_{max,gas}} = \frac{C(\varepsilon - 1)}{(2\varepsilon + 1)} \quad (1)$$

In this equation, $\lambda_{max,\ gas}$ and $\lambda_{max,\ solution}$ are the wavelength of most intensity electronic transition of complex in the gas phase and solution phase, respectively, ε is the dielectric constant of the solvent, and C is a constant depending on the dimensions and electrical properties of the solute dipole. The similar equations are considered for NMR calculations.

Analysis spectra analysis of the investigated molecules were done using time-dependent-DFT method (TD-DFT)[62] by identical level of theory as applied to calculate the optimization. The 20 minimum excitation energies were evaluated.

The percentage contributions of atomic orbitals in the frontier orbitals were calculated via GaussSum 3.0 software package.[63]

Natural Transition Orbital (NTO) analysis[64] was accomplished by means of the TD-DFT results. NTO analysis and the corresponding plots were provided using the Multiwfn 3.5 package.[58]

Shielding values of ^{119}Sn nucleus was calculated at the B3LYP/ZORA-def2-TZVP(-f)[65] level of theory, using the scalar all-electron zeroth-order regular approximation (ZORA)[66] to treat relativistic effects. Calculations utilized the SARC/J auxiliary basis.[67-71] Chemical shift values were computed using the Gauge independent atomic orbital (GIAO) method.[72] NMR calculations were run in ORCA (Version 4.0.0).[73]

3. RESULTS AND DISCUSSION

Energetic aspects

The structure of the investigated carbene complex of stannocene is presented in Figure 1. Energy values of this complex are computed in gas and various solvents by the CPCM method (Table 1). Three protic and three aprotic solvents considered in this study. Aprotic solvents are chloroform, n-hexane, and pyridine. On the other hand, protic solvents include water, methanol, and ethanol. Dielectric constant and refractivity of these solvents are listed in Table 1.[74] The various dielectric constants reveal different field strengths.

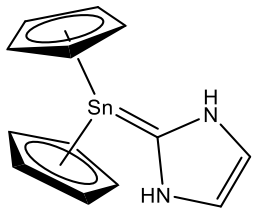

Figure 1. The structure of Cp_2Sn=NHC complex.

It can be found that the complex was more stable in more polar solvents. The solvation energy (E_{solv}) values of the carbene complex of stannocene are collected in Table 1. The negative values of E_{solv} illustrate that the carbene complex of stannocene is more stable in solution phase than gas phase. The E_{solv} values decrease in the presence of more polar solvents.

Table 1. Total energy (E, a.u), solvation energy (E_{solv}, kcal mol^{-1}) and dipole moment (μ, Debye) values of the Cp_2Sn=NHC complex in the gas and solution phases. ε and n_D are dielectric constant and refractivity of these solvents, respectively

	ε	n_D	E	E_{solv}	μ
Gas	-	-	-827.6540	0.00	8.30
Aprotic					
n-Hexane	1.88	1.38	-827.6634	-5.87	10.05
Chloroform	4.71	1.45	-827.6716	-11.01	11.69
Pyridine	12.30	1.51	-827.6757	-13.61	12.49
Protic					
Ethanol	24.30	1.36	-827.6770	-14.43	12.76
Methanol	32.63	1.33	-827.6773	-14.63	12.82
Water	78.54	1.33	-827.6779	-15.02	12.95

Dipole moment

Dipole moment values of the studied complex are calculated in gas and various solvents (Table 1). The calculated values indicate the larger dipole moment values in solution phase than gas phase. It can be observed, the larger values in the presence of more polar solvents. Higher dipole moment values are due to long range interactions of solvent with the solute molecules.

Linear correlation between dipole moment values and dielectric constant of solvent display this equation:

$$\mu = 0.0251\ \varepsilon + 11.479; \qquad R^2 = 0.4091$$

so, the good linear relationship between these parameters was not observed.

Various investigations have been reported about the linear correlations between the dipole moment of the molecules and solvent polarity functions, which commonly consider both the refractive index[61] and the dielectric constant of the liquid medium.

In this study, we utilize the Lippert-Mataga polarity function (called orientation polarizability of the solvent),[75,76] Bakhshiev polarity function[77] and to Bilot and Kawski.[78] These functions have the equations of:

Lippert-Mataga polarity function:

$$F_{LM}(\varepsilon,n)=\frac{\varepsilon-1}{2\varepsilon+1}-\frac{n^2-1}{2n^2+1} \quad (2)$$

Bakhshiev polarity function:

$$F_B(\varepsilon,n)=\frac{2n^2+1}{n^2+2}-\left(\frac{\varepsilon-1}{\varepsilon+2}-\frac{n^2-1}{n^2+2}\right) \quad (3)$$

Bilot and Kawski function:

$$F_{BK}(\varepsilon,n)=\frac{2n^2+1}{2(n^2+2)}\left(\frac{\varepsilon-1}{\varepsilon+2}-\frac{n^2-1}{n^2+2}\right)+\frac{3(n^4-1)}{2(n^2+2)^2} \quad (4)$$

The linear correlations between μ and these solvent polarity functions are:

$\mu = 8.7996\ F_{LM}(\varepsilon,n) + 10.259$; $R^2 = 0.9598$

$\mu = 3.0851\ F_{B}(\varepsilon,n) + 10.286$; $R^2 = 0.9630$

$\mu = 6.5746\ F_{BK}(\varepsilon,n) + 7.9888$; $R^2 = 0.9886$

It can be seen, there is a better correlation between the dipole moment and Bilot and Kawski function in the carbene complex of stannocene complex. Consequently, this model indicates a better linear correlation between dipole moment values and solvent polarity functions which took into account the dielectric constant and refractive index.

Molecular orbital analysis

Frontier orbital energy and HOMO-LUMO gap values of this complex are calculated in gas and various solvents (Table 3). It can be seen, larger HOMO-LUMO gap in solution phase than gas phase. The corresponding is larger in the presence of more polar solvents.

On the other hand, E(HOMO) and E(LUMO) values reveal that more stabilities of the HOMO and LUMO in solution phase than gas phase. In the solvent, particularly polar solvents, could indeed impact the geometry through long range interactions with the solute molecules hence stabilizing their frontier molecular orbitals.a A good linear correlation between HOMO-LUMO gap values and E_{solv} values can be seen (Figure 2):

$E_{solv} = -32.955\ Gap + 155.98$; $R^2 = 0.9800$

The hardness (η) and chemical potential (μ) values are calculated by the following equations:

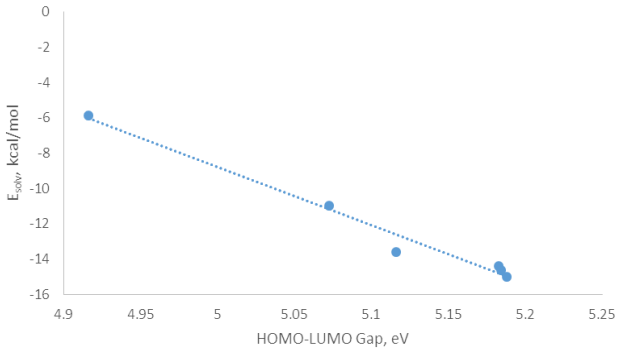

Figure 2. Linear correlation between HOMO-LUMO gap values and E_{solv} values of Cp_2Sn=NHC complex in studied solvents.

Table 2. Frontier orbitals energy (eV), HOMO-LUMO gap (eV), Hardness (η, eV), chemical potential (μ, eV) and electrophilicity (ω, eV) values of the Cp_2Sn=NHC complex in the gas and solution phases

	E(HOMO)	E(LUMO)	Gap	η	μ	ω
Gas	-5.436	-0.586	4.850	2.425	-3.011	1.870
Aprotic						
n-Hexane	-5.562	-0.645	4.917	2.458	-3.103	1.959
Chloroform	-5.664	-0.590	5.073	2.537	-3.127	1.927
Pyridine	-5.725	-0.608	5.117	2.558	-3.167	1.960
Protic						
Ethanol	-5.738	-0.555	5.183	2.592	-3.147	1.910
Methanol	-5.743	-0.558	5.185	2.592	-3.151	1.915
Water	-5.753	-0.565	5.188	2.594	-3.159	1.923

$$\eta=\frac{E(LUMO)-E(HOMO)}{2} \quad (5)$$

$$\mu=\frac{E(HOMO)+E(LUMO)}{2} \quad (6)$$

It can be noticed that the values of global reactivity descriptors (η and μ) of the complex increase in going from gas phase to the solvent medium (Table 2). The variations are more for protic solvents than for the aprotic ones.

Figure 3 presents plots of frontier orbitals in the Cp_2Sn=NHC complex. It can be observed, there is significance π-bonding between Sn and $C_{carbene}$ in the LUMO. The calculated percentage contributions of atomic orbitals in the HOMO are 97% (Cp) and 3% (Sn). The corresponding values for LUMO are 16% (Cp), 53% (NHC) and 31% (Sn). It can be observed, the most contribution percent values belong to Cp and NHC ligand in the HOMO and LUMO, respectively.

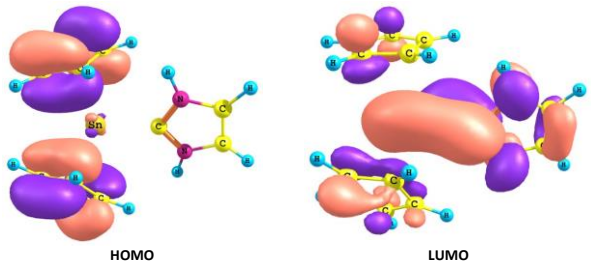

Figure 3. Plots of frontier orbitals of Cp_2Sn=NHC complex.

Table 3. Calculated Hirshfeld charge of the selected atoms of the neutral, cationic and anionic states of the Cp_2Sn=NHC complex in the gas and solution phases

Neutral							
	Gas	Aprotic				Protic	
Atom		n-Hexane	Chloroform	Pyridine	Ethanol	Methanol	Water
Sn	0.2756	0.2523	0.2330	0.2256	0.2231	0.2226	0.2216
$C_{carbene}$	-0.0298	-0.0225	-0.0150	-0.0125	-0.0105	-0.0104	-0.0101
N	-0.0309	-0.0253	-0.0201	-0.0176	-0.0166	-0.0164	-0.0160
N'	-0.0315	-0.0256	-0.0203	-0.0178	-0.0175	-0.0173	-0.0169
C	-0.0158	-0.0101	-0.0053	-0.0026	-0.0018	-0.0016	-0.0012
C'	-0.0157	-0.0099	-0.0053	-0.0027	-0.0023	-0.0021	-0.0017

Anion							
	Gas	Aprotic				Protic	
Atom		n-Hexane	Chloroform	Pyridine	Ethanol	Methanol	Water
Sn	0.0604	-0.0096	-0.1157	-0.1630	-0.1867	-0.1897	-0.1956
$C_{carbene}$	-0.1154	-0.0997	-0.0569	-0.0478	-0.0341	-0.0339	-0.0337
N	-0.0727	-0.0627	-0.0395	-0.0319	-0.0252	-0.0249	-0.0242
N'	-0.0754	-0.0685	-0.0548	-0.0507	-0.0486	-0.0485	-0.0481
C	-0.0594	-0.0483	-0.0289	-0.0204	-0.0143	-0.0137	-0.0127
C'	-0.0559	-0.0455	-0.0275	-0.0208	-0.0164	-0.0161	-0.0154

Cation							
	Gas	Aprotic				Protic	
Atom		n-Hexane	Chloroform	Pyridine	Ethanol	Methanol	Water
Sn	0.3239	0.3104	0.2991	0.2961	0.2946	0.2945	0.2941
$C_{carbene}$	-0.0399	-0.0278	-0.0171	-0.0129	-0.0107	-0.0104	-0.0099
N	-0.0269	-0.0215	-0.0164	-0.0137	-0.0127	-0.0125	-0.0122
N'	-0.0261	-0.0205	-0.0151	-0.0126	-0.0121	-0.0119	-0.0115
C	0.0037	0.0044	0.0048	0.0055	0.0056	0.0056	0.0058
C'	0.0045	0.0050	0.0051	0.0055	0.0052	0.0053	0.0054

Condensed Fukui function and condensed dual descriptor

The variation in electron density though addition or eliminating an electron, as the condensed Fukui function (CFF) around an atom, indicates the reactivity pattern of that atom. The solvent medium changes the reactivity of the molecules in gas phase. In this situation, the electron density would be redistributed in the presence of the solvents and the reactivity would be revealed with CFF. The most reactive atoms of molecule are considered to illustration of reactivity descriptors of atoms in the molecules. Various approaches have been reported to calculate atomic charges. Yet, Hirshfeld charge is established to be very suitable for this resolve. Some studies have illustrated that Hirshfeld charge can be successfully working to explore reactive sites in terms of condensed Fukui function.[79-81] Calculated Hirshfeld charge of the selected atoms of the neutral, cationic and anionic states of the Cp_2Sn=NHC complex are gathered in Table 3 in the gas and solution phases.

The CFF values (f^+ and f^-) are presented in Table 4. For example, the electrophilic CFF is highest for Sn and the nucleophilic CFF is the highest for $C_{carbene}$ atom in both cases. The CFF for nucleophilic attack for Sn atom (i.e., the electrophilicity of Sn atom) increases as we move on from gas phase to solvent medium with increasing the dielectric constant of the solvent medium (Table 4). Likewise, in going from gas phase to solvent medium and increasing the dielectric constant of the solvent medium, the CFF for electrophilic attack for $C_{carbene}$ atom (i.e., the nucleophilicity of $C_{carbene}$ atom) also decreases (Table 4).

Again, it is to be pointed out that the change in the reactivity, either the electrophilicity of Sn atom or the nucleophilicity of Table 4 atom, is significant for the aprotic solvents (Table 4). The change in protic solvent with high dielectric constant, ranging from 24.3 for ethanol to 78.54 for water, does not affect either the electrophilicity of Sn atom or the nucleophilicity of $C_{carbene}$ atom in the complex (Table 4).

^{119}Sn NMR

The Isotropic chemical shift of the ^{119}Sn nucleus in the $SnMe_4$ ($\delta_{reference}$), Cp_2Sn=NHC complex ($\delta_{complex}$) and relative chemical shift (δ) values in the gas and solution phases are gathered in Table 5. The corresponding value places at -1700.256 ppm in gas phase. The calculated values reveal that good compatible experimental results in the similar complexes.[21]

These values indicate the larger chemical shift values in various solvents than gas phase. These computed values are larger in the more polar solvents. These solvent-induced chemical shifts reveal that the shielding constant of a nucleus in a particular molecule is dependent on the electronic distribution within the molecule and the character of the surrounding medium.[61]

Table 4. Condensed Fukui function (f^- and f^+) of the Cp_2Sn=NHC complex in gas and solution

				f^+			
	Gas	Aprotic				Protic	
Atom		n-Hexane	Chloroform	Pyridine	Ethanol	Methanol	Water
Sn	-0.0483	-0.0581	-0.0662	-0.0705	-0.0716	-0.0719	-0.0725
$C_{carbene}$	0.0101	0.0053	0.0021	0.0004	0.0002	0.0000	-0.0002
N	-0.0040	-0.0039	-0.0038	-0.0038	-0.0039	-0.0039	-0.0039
N'	-0.0054	-0.0051	-0.0052	-0.0052	-0.0054	-0.0054	-0.0054
C	-0.0196	-0.0145	-0.0100	-0.0080	-0.0074	-0.0072	-0.0069
C'	-0.0202	-0.0149	-0.0103	-0.0082	-0.0076	-0.0074	-0.0071

				f^-			
	Gas	Aprotic				Protic	
Atom		n-Hexane	Chloroform	Pyridine	Ethanol	Methanol	Water
Sn	0.0483	0.0581	0.0662	0.0704	0.0716	0.0719	0.0725
$C_{carbene}$	-0.0101	-0.0053	-0.0021	-0.0004	-0.0002	0.0000	0.0002
N	0.0040	0.0039	0.0038	0.0038	0.0039	0.0039	0.0039
N'	0.0054	0.0051	0.0052	0.0052	0.0054	0.0054	0.0054
C	0.0196	0.0145	0.0100	0.0080	0.0074	0.0072	0.0069
C'	0.0202	0.0149	0.0103	0.0082	0.0075	0.0074	0.0071

Table 5. Isotropic chemical shift of the ^{119}Sn nucleus in the $SnMe_4$ ($\delta_{reference}$, ppm), Cp_2Sn=NHC complex ($\delta_{complex}$, ppm) and relative chemical shift (δ, ppm) values in the gas and solution phases

	$\delta_{complex}$	$\delta_{reference}$	$\delta=\delta_{reference}-\delta_{complex}$
Gas	4239.39	2539.13	-1700.26
Aprotic			
n-Hexane	3958.83	2553.80	-1405.03
Chloroform	3757.85	2565.28	-1192.57
Pyridine	3675.40	2569.83	-1105.57
Protic			
Ethanol	3647.08	2571.34	-1075.74
Methanol	3641.61	2571.78	-1069.83
Water	3629.43	2572.48	-1056.95

The dependency of values of chemical shifts on dielectric constant of solvents has been investigated, and there are not good relationships between these shifts values and dielectric constant:

$$\delta(^{119}Sn) = 2.9139\ \varepsilon - 1225.9; \qquad R^2 = 0.3826$$

Dependency of the chemical shift values of ^{119}Sn atom in the studied complex versus (ε - 1)/(2ε + 1) of KBM equation exhibits a linear relationship between these chemical shift values and KBM parameters. These equations are as follows:

$$\frac{\Delta\delta}{\delta_{gas}} = -0.6697\frac{\varepsilon-1}{Z\varepsilon+1} - 0.0529;\ R^2 = 0.9$$

The regression coefficients using the data for investigated solvents systems are shown for ^{119}Sn NMR chemical shift values of complex in the following equation:

$$\frac{\Delta\delta}{\delta_{gas}} = -0.02254 - 0.6745\frac{\varepsilon-1}{2\varepsilon+1} - 0.3567\frac{n^2-1}{2n^2+1};\ R^2 = 0.9987$$

Therefore, solvent-induced chemical shifts changes reveal a good linear relationship with modified-KBM equation.

Electronic transitions

The wavelengths of the strongest absorption band ($\lambda_{max,el}$) of the singlet ground state of the carbene complex of stannocene are collected in Table 6 for gas and solution phases. It can be found, the larger $\lambda_{max,el}$ values in the gas phase than solution phase.

Table 6. The wavelength (λ_{max}, nm) and oscillator strength (f) of the strongest absorption band values of the Cp_2Sn=NHC complex in the gas and solution phases.

	λ_{max}	f
Gas	220.14	0.1214
Aprotic		
n-Hexane	218.20	0.2252
Chloroform	212.58	0.1051
Pyridine	210.40	0.1286
Protic		
Ethanol	211.48	0.1541
Methanol	211.25	0.1608
Water	210.92	0.1767

As shown, the $\lambda_{max,el}$ values are blue shifted by increasing the solvent polarity. According to the occurred solvent-induced $\lambda_{max,el}$ changes, values depend on the electronic distribution within the molecule and the characteristics of the surrounding medium.[74]

Linear correlation between λ_{max} values and dielectric constant of solvent show the following equations:

$$\lambda_{max,el} = -2.0 \times 10^{-4}\ \varepsilon - 0.0301;\ R^2 = 0.2377$$

It can be seen, there is not good linear correlation between these parameters.

Dependency of the $\lambda_{max,el}$ values in the studied carbene complex versus (ε - 1)/(2ε + 1) of KBM equation exhibits a linear relationship between these $\lambda_{max,el}$ values and KBM parameters. These equations are as follows:

$$\frac{\Delta\lambda_{max,el}}{\lambda_{max,gas,el}} = -0.1073\frac{(\varepsilon-1)}{(2\varepsilon+1)} + 0.0085;\ R^2 = 0.9146$$

The regression coefficients using the data for investigated solvents systems are shown for λ_{max} values of the complex in the following equation:

$$\frac{\Delta\lambda_{max,el}}{\lambda_{max,gas,el}} = 0.04967 - 0.1138\,\frac{\varepsilon-1}{2\varepsilon+1} - 0.4839\,\frac{n^2-1}{2n^2+1};\ R^2 = 0.9922$$

Thus, solvent-induced $\lambda_{max,el}$ values changes indicated a good linear relationship with the modified-KBM equation.

Natural transition orbitals (NTOs) analysis

Excited state calculated for this absorption band is not pure states that correspond to a unique electronic transition between molecular orbitals, but they are rather a combination of several electronic transitions.

For the purpose of exploring the nature of the strongest absorption band for in the studied complex, here we provided the natural transition orbitals (NTOs). In the gas phase, the highest 10 eigenvalues of occupied NTOs:

0.000200 0.000289 0.000340 0.000457 0.001142
0.004202 0.019948 0.068388 0.297509 0.608343

The highest 10 eigenvalues of virtual NTOs:

0.608343 0.297509 0.068388 0.019948 0.004202
0.001142 0.000457 0.000340 0.000289 0.000200

It can be seen that, the eigenvalues of occupied and virtual NTOs have one-to-one correspondence, the largest eigenvalue is 0.608343, which means that NTO pair contributes as high as 60.83% of the $S_0 \rightarrow S_{20}$ transition.

The dominant "particle"-"hole" contribution for the corresponding of the complex are plotted in Figure 4. The electron density of the hole NTO for the studied complex is localized on the Cp ligands. On the contrary, the electron density of the particle NTOs is localized mainly on the Sn and NHC moiety. This indicates that photo-induced charge transfer is highly likely taken place for this complex.

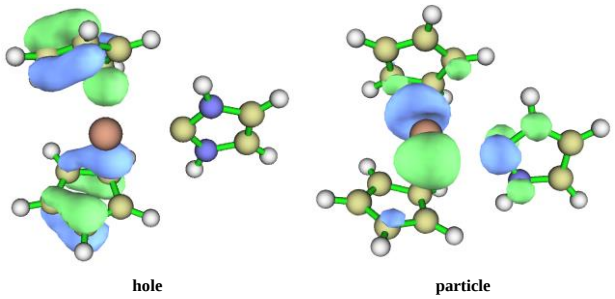

Figure 4. Natural transition orbitals (NTOs) of the corresponding excited state of the most intensity transition in the Cp_2Sn=NHC complex.

4. CONCLUSION

In this work, the influence of solvent polarity on structure, electronic properties, electronic spectrum and ^{119}Sn NMR parameters of Cp_2Sn=NHC complex was investigated using the MPW1PW91 method. According to the computations, the solvation energy values indicated enhanced stability of the title complex in protic solvents than aprotic solvents. Also, good correlation was observed between dipole moment and Bilot and Kawski function. The values of global reactivity descriptors, the chemical potential and hardness values of the complex were increased in going from gas phase to the solvent medium. Good linear correlations were also detected between ^{119}Sn chemical shift values and KBM solvent parameters. NTO results revealed that photo-induced charge transfer was highly likely taken place for this complex.

CONFLICTS OF INTEREST

There are no conflicts to declare.

AUTHOR INFORMATION

Corresponding Author(s)

Reza Ghiasi: Email: rezaghiasi1353@yahoo.com, *ORCID*: 0000-0002-1200-6376

Author(s)

Simin Samavat, Bita Mohtat

REFERENCES

1. A. J. Arduengo, R. L. Harlow, M. Kline, *J. Am. Chem. Soc.*, **1991**, *113*, 361-363.
2. H. -W. Wanzlick, E. Schikora, *Angew. Chem.*, **1960**, *72*, 494-494.
3. H. -W. Wanzlick, E. Schikora, *Chem. Ber.*, **1961**, *94*, 2389-2393.
4. M. N. Hopkinson, C. Richter, M. Schedler, F. Glorius, *Nature*, **2014**, *510*, 485-496.
5. T. Dröge, F. D. M. Glorius, *Angew. Chem.*, **2010**, *122*, 7094-7107.
6. S. M. N. Díez-Gonzalez, S. P. Nolan, *Chem. Rev.*, **2009**, *109*, 3612-3676.
7. C. E. Willans, *in Organometallic Chemistry, The Royal Society of Chemistry*, **2010**, *36*, 1-28.
8. S. Wurtemberger-Pietsch, U. Radius, T. B. Marder, *Dalton Trans.*, **2016**, *45*, 5880-5895.
9. M. Soleilhavoup, G. Bertrand, *Acc. Chem. Res.*, **2015**, *48*, 256-266.
10. G. Frenking, M. Hermann, D. M. Andrada, N. Holzmann, *Chem. Soc. Rev.* , **2016**, *45*, 1129-1144.
11. B. Gehrhus, B. H. P, M. F. Lappert, *J. Chem. Soc., Dalton Trans.*, **2000**, 3094-3099.
12. F. Stabenow, W. Saak, M. Weidenbruch, *Chem. Commun.*, **1999**, 1131-1132.
13. S. M. I. Al-Rafia, R. McDonald, M. J. Ferguson, E. Rivard, *Chem. -Eur. J.*, **2012**, *18*, 13810-13820.
14. P. A. Rupar, M. C. Jennings and K. M. Baines, *Can. J. Chem.*, **2007**, *85*, 141−147.
15. S. M. I. Al-Rafia, A. C. Malcolm, S. K. Liew, M. J. Ferguson, E. Rivard, *J. Am. Chem. Soc.*, **2011**, *133*, 777-779.

16. H. Grützmacher, S. Freitag, R. M. Herbst-Irmer, G. M. Sheldrick, *Angew. Chem*., **1992**, *104*, 459-461.
17. N. Kuhn, A. Al-Sheikh, *Coord. Chem. Rev*., **2005**, *249*, 829-857.
18. A. J. Arduengo, F. Davidson, R. Krafczyk, W. J. Marshall, M. Tamm, *Organometallics*, **1998**, *17*, 3375-3382.
19. M. A. Beswick, N. L. Cromhout, C. N. Harmer, P. R. Raithby, C. A. Russell, J. S. B. Smith, A. Steiner and D. S. Wright, *Chem. Commun.*, **1996**, 1977-1978.
20. D. R. Armstrong, M. A. Beswick, N. L. Cromhout, C. N. Harmer, D. Moncrieff, C. A. Russell, P. R. Raithby, A. Steiner, A. E. H. Wheatley, D. S. Wright, *Organometallics*, **1998**, *17*, 3176-3181.
21. C. Müller, A. Stahlich, L. Wirtz, C. Gretsch, V. Huch, A. Schäfer, *Inorg. Chem*., **2018**, *57*, 8050-8053.
22. S. Danés, C. Müller, L. Wirtz, V. Huch, T. Block, R. Pöttgen, A. Schäfer, D. M. Andrada, *Organometallics*, **2020**, *39*, 516-527.
23. P. Selvarengan, P. Kolandaivel, *J. Mol. Struct*.: THEOCHEM, **2002**, *617*, 99-106.
24. S. B. Allin, T. M.Leslie, R. S. Lumpkin, *Chem. Mater*. **1996**, *8*, 428.
25. A. J. A. Aquino, D. Tunega, G. Haberhauer, M. H. Gerzabek, H. Lischka, *J. Phys. Chem. A*, **2002**, *106*, 1862-1871.
26. J. Tomasi, B. Mennucci, R. Cammi, *Chem. Rev.*, **2005**, *105*, 2999-3094.
27. M. Springborg, Specialist Periodical Reports: Chemical Modelling, Applications and Theory, Royal Society of Chemistry, Cambridge, UK, **2008**.
28. A. Taha, O. M. I. Adly, M. Shebl, *Spectrochim. Acta A Mol. Biomol.* **2015**, *140*, 74-84.
29. R. E. Skyner, J. L. McDonagh, C. R. Groom, T. V. Mourika, J. B. O. Mitchell, *Phys.Chem.Chem.Phys.*, **2015**, *17*, 6174-6191.
30. R. Kar, S. Pal, *Int. J. Quantum Chem.*, **2010**, *110*, 1642-1647.
31. B. Jovića, A. Nikolića, S. Petrovićb, B. Kordića, T. Đaković-Sekulića, N. Stojanović, *Struct. Chem.*, **2014**, *55*, 1616-1622.
32. Y. -K. Li, H. -Y. Wu, Q. Zhu, K. -X. Fu, X. -Y. Li, *Comput. Theor. Chem.* **2011**, *971*, 65-72.
33. J. Basavaraja, S. R. Inamdar, H. M. S. Kumar, *Spectrochim. Acta A Mol. Biomol.* **2015**, *137*, 527-534.
34. G.Ersan, O. G. Apul, T. Karanfil, *Water Research* **2016**, *98*, 28-38.
35. Y. Ouennoughi, H. E. Karce, D. Aggoun, T. Lanez, E. Morallon, *J. Organomet. Chem.* **2017**, *848*, 344-351.
36. M. Aydin, D. L. Akins, *Comput. Theor. Chem.* **2018**, *1132*, 12-22.
37. C. -L. Wu, S. -H. Zhang, R. -J. Gou, F. -D. Ren, S. -F. Zhu, *Comput. Theor. Chem.* **2018**, *1127*, 22-30.
38. H. F. Dos Santos, M. A. Chagas, L. A. De Souza, W. R. Rocha, M. V. De Almeida, C. P. A. Anconi, W. B. De Almeida, *J. Phys. Chem. A*, **2017**, *121*, 2839-2846.
39. M. Ganesan, N. Vedamanickam, S. Paranthaman, *Comput. Theor. Chem.* **2018**, *17*, 1850009.
40. D. Shen, P. Su, W. Wu, *Phys. Chem. Chem. Phys.*, **2018**, *20*, 26126-26139.
41. T. -J. Bi, L. -K. Xu, F. Wang, X. -Y. Li, *Phys. Chem. Chem. Phys*., **2018**, *20*, 13178-13190.
42. O. V. Sizova, N. V. Ivanova, O. O. Lyubimova, V. V. Sizov, *Russ. J. Coord. Chem.*, **2007**, *33*, 523-529.
43. R. S. Shamsiev, A. V. Drobyshev, *Russ. J. Inorg. Chem.*,**2013**, *58*, 1506-1510.
44. N. N. Milani, R. Ghiasi, A. Forghaniha, *J. Appl. Chem. Spect.*, **2020**, *86*, 1123-1131.
45. M. J. Frisch, G. W. Trucks, H. B. Schlegel, G. E. Scuseria, M. A. Robb, J. R. Cheeseman, G. Scalman, V. Barone, B. Mennucci, G. A. Petersson, H. Nakatsuji, M. Caricato, X. Li, H. P. Hratchian, A. F. Izmaylov, J. Bloino, G. Zheng, J. L. Sonnenberg, M. Hada, M. Ehara, K. Toyota, R. Fukuda, J. Hasegawa, M. Ishida, T. Nakajima, Y. Honda, O. Kitao, H. Nakai, T. Vreven, J. A. Montgomery, Jr., J. E. Peralta, F. Ogliaro, M. Bearpark, J. J. Heyd, E. Brothers, K. N. Kudin, V. N. Staroverov, R. Kobayashi, J. Normand, K. Raghavachari, A. Rendell, J. C. Burant, S. S. Iyengar, J. Tomasi, M. Cossi, N. Rega, J. M. Millam, M. Klene, J. E. Knox, J. B. Cross, V. Bakken, C. Adamo, J. Jaramillo, R. Gomperts, R. E. Stratmann, O. Yazyev, A. J. Austin, R. Cammi, C. Pomelli, J. W. Ochterski, R. L. Martin, K. Morokuma, V. G. Zakrzewski, G. A. Voth, P. Salvador, J. J. Dannenberg, S. Dapprich, A. D. Daniels, O. Farkas, J. B. Foresman, J. V. Ortiz, J. Cioslowski, D. J. Fox, Gaussian, Inc., Wallingford CT, Revision A.02 edn., **2009**.
46. P. J. Hay, *J. Chem. Phys*., **1977**, *66*, 4377-4384.
47. R. Krishnan, J. S. Binkley, R. Seeger, J. A. Pople, *J. Chem. Phys*., **1980**, *72*, 650-654.
48. A. D. McLean, G. S. Chandler, *J. Chem. Phys.*, **1980**, *72*, 5639-5648.
49. A. J. H. Wachters, *J. Chem. Phys*., **1970**, *52*, 1033-1036.
50. D. Rappoport, F. Furche, *J. Chem. Phys*., **2010**, *133*, 134105.
51. D. Andrae, U. Haeussermann, M. Dolg, H. Stoll, H. Preuss, *Theor. Chim. Acta*, **1990**, *77*, 123-141.
52. C. Adamo, V. Barone, *J. Chem. Phys*., **1998**, *108*, 664-675.
53. R. C. Dunbar, *J. Phys. Chem. A*, **2002**, *106*, 7328-7337.
54. M. Porembski, J. C. Weisshaar, *J. Phys. Chem. A*, **2001**, *105*, 6655-6667.

55. M. Porembski, J. C. Weisshaar, *J. Phys. Chem. A*, **2001**, *105*, 4851-4864.
56. Y. Zhang, Z. Guo, X. -Z. You, *J. Am. Chem. Soc.*, **2001**, *123*, 9378-9387.
57. F. L. Hirshfeld, *Theor. Chim. Acta* **1977**, *44*, 129-138.
58. T. Lu, F. Chen, *J. Comp. Chem.*, **2012**, *33*, 580-592.
59. V. Barone, M. Cossi, *J. Phys. Chem. A*, **1998**, *102*, 1995-2001.
60. M. Cossi, N. Rega, G. Scalmani, V. Barone, *J. Comp. Chem.*, **2003**, *24*, 669-681.
61. C. Reichardt, T. Welton, Solvents and Solvent E¤ects in Organic Chemistry, WILEY-VCH Verlag GmbH & Co. KGaA, Weinheim, Fourth Edition edn., **2011**.
62. E. Runge, E. K. U. Gross, *Phys. Rev. Lett.*, **1984**, *52* 997-1000.
63. N. M. O'Boyle, A. L. Tenderholt, K. M. Langer, *J. Comput. Chem.*, **2008**, *29*, 839-845.
64. R. L. Martin, *J. Chem. Phys.*, **2003**, *118*, 4775-4777.
65. F. Weigend, R. Ahlrichs, *Phys. Chem. Chem. Phys.*, **2005**, *7*, 3297-3305.
66. E. V. Lenthe, E. J. Baerends, J. G. Snijders, *J. Chem. Phys.*, **1993**, *99*, 4597-4610.
67. F. Weigend, *Phys. Chem. Chem. Phys.*, **2006**, *8*, 1057-1065.
68. D. A. Pantazis, F. Neese, *J. Chem. Theory Comput.*, **2009**, *5*, 2229-2238.
69. D. A. Pantazis, X. Y. Chen, C. R. Landis, F. Neese, *J. Chem. Theory Comput.*, **2008**, *4*, 908-919.
70. D. A. Pantazis, F. Neese, *Theor. Chem. Acc.*, **2012**, *131*, 1292.
71. D. A. Pantazis, F. Neese, *J. Chem. Theory Comput.*, **2011**, *7*, 677-684.
72. K. Wolinski, J. F. Hinton, P. Pulay, *J. Am. Chem. Soc.* , **1990**, *112*, 8251-8260.
73. F. Neese, *WIREs Comput. Mol. Sci.*, **2017**, *8*, e1327.
74. C. Reichardt, T. Welton, Solvents and Solvent Effects in Organic Chemistry, WILEY-VCH Verlag GmbH & Co. KGaA, Weinheim, Fourth edn., **2011**.
75. E. Lippert, *Zeitschrift für Naturforschung A*, **1955**, *10*, 541-545.
76. N. Mataga, Y. Kaifu, M. Koizumi, *Bull. Chem. Soc. Jpn.*, **1956**, *29*, 465-470.
77. N. G. Bakhshiev, *Opt. Spektrosk*, **1964**, *16*, 821-832.
78. L. Bilot, A. Kawski, Z. Naturforsch, *Zeitschrift für Naturforschung A*, **1962**, *17a*, 621-627.
79. C. J. Oláh, V. Alsenoy, A. B. Sannigrahi, *J. Phys. Chem. A.*, **2002**, *106*, 3885-3890.
80. S. Liu, C. Rong, T. Lu, *J. Phys. Chem. A.*, **2014**, *118*, 3698-3704.
81. R. K. Roy, *J. Phys. Chem. A.*, **2003**, *107*, 10428-10434.